

Simulation of a two-dimensional Rayleigh-Bénard system using the direct simulation Monte Carlo method

Tadashi Watanabe, Hideo Kaburaki, and Mitsuo Yokokawa
*Computing and Information Systems Center, Japan Atomic Energy Research Institute,
Tokai-mura, Naka-gun, Ibaraki-ken, 319-11, Japan*

(Received 13 December 1993)

The transition from conduction to convection in the two-dimensional Rayleigh-Bénard system has been simulated using the direct simulation Monte Carlo method, where the diffuse reflection boundary conditions are strictly applied at the top and bottom walls. It is shown that the determined critical Rayleigh number agrees well with that obtained by the macroscopic hydrodynamic equations.

PACS number(s): 47.20.Bp, 47.27.Te, 05.70.Ln

I. INTRODUCTION

The direct simulation Monte Carlo (DSMC) method is one of the most widely used numerical techniques for simulating rarefied gas flows with incorporating atomistic details. This technique was originally developed by Bird [1] and has been applied to various types of flow problems. In this method, a large number of molecules in a real gas are simulated by a smaller number of representative particles. The trajectories of these particles are traced in a short time interval by decoupling interparticle collisions and taking interactions with boundaries into account. Interparticle collisions take place on a probabilistic basis in a collision cell. Macroscopic quantities are obtained by sampling particle properties in a sampling cell, which is generally larger than the collision cell.

The macroscopic hydrodynamic phenomenon of the vortex shedding past an inclined flat plate in the near-continuum region was studied by Meiburg [2] using both the molecular-dynamics (MD) method and the DSMC method. A vortex street was not observed in the DSMC results because the size of the collision cell in this simulation was about three times larger than the mean free path. This was pointed out by Bird [3] using the forced vortex in a lid-driven cavity flow. He suggested that the size of the collision cell must be small in comparison with the mean free path. Koura [4] has also studied the process of vortex shedding past an inclined flat plate and concluded that large-scale vortices were observed with the collision cell size considerably greater than the mean free path on the condition that an average number of particles per cell was sufficiently large. Kaburaki and Yokokawa [5] calculated the forced vortex in a lid-driven cavity flow in the continuum region abiding strictly by the criterion of the number of particles for the Bird method and found that the DSMC results were in good agreement with the results by the Navier-Stokes equation. Through these studies, the DSMC method was found to be able to predict vortices in a flow field.

Besides the flow field simulations, the DSMC method has been applied to the simulation of the temperature fields. Garcia [6] has studied the heat conduction in a dilute gas. The steady-state temperature gradient was eval-

uated between the parallel flat plates with different temperatures, and the temperature distribution in the heat conduction state was shown to be predicted by the DSMC method.

The Rayleigh-Bénard (RB) system, in which both the heat conduction and the vortex formation play an important role, has been studied by many researchers experimentally [7] and numerically [8]. In the RB system, when the temperature difference between the top and bottom walls exceeds the critical value, the transition from conduction to convection occurs, which is known as the RB instability.

The RB convection has also been studied at the molecular level since the microscopic fluctuations of field variables would result in flow instability. Mareschal and Kestemont [9] have shown the RB convection rolls by using the MD method when the Rayleigh number was much higher than the critical Rayleigh number. Rapaport [10] reported the occurrence of the transient roll patterns with higher wave number during the development of the stable RB convection by the MD method. Mareschal *et al.* [11], Puhl, Mansour, and Mareschal [12], and Given and Clementi [13] compared the field variables obtained by the MD method with the results by the hydrodynamic calculation. Garcia [14] studied the RB convection rolls by using the DSMC method and Garcia and Penland [15] compared the DSMC results with the numerical solution of the Navier-Stokes equations. Although the convection rolls were observed and the field variables were discussed in these MD and DSMC simulations, these works all employed semislip boundary conditions at the top and bottom walls of the system. Two types of semislip boundary conditions were applied: in Refs. [9], [11], and [12], only the velocity component in the perpendicular direction to the wall is thermalized according to the Maxwellian distribution with the surface temperature and the transverse component unchanged, while in Refs. [10] and [13], the perpendicular component is simply reversed and all the components are scaled to match the surface temperature. It is thus clear that the semislip boundary condition does not satisfy the Maxwellian distribution completely at the wall, and the simulated flow field might be affected.

Stefanov and Cercignani [16] have shown that the convection rolls could be formed by using the diffuse reflection boundary condition, in which the incident particle loses its thermal property completely and appears with the velocity components randomly sampled from the Maxwellian distribution corresponding to the temperature of the surface. The influence of the boundary condition upon the field variables was, however, not discussed. In any case, the transition from the conduction to the convection state has not yet been clearly predicted at the molecular level both by the MD and the DSMC methods.

In this study the DSMC method of Bird [1] is applied to the RB system to predict the critical Rayleigh number at which the RB instability occurs. The effect of the boundary condition on the critical Rayleigh number is discussed.

II. DSMC SIMULATION

The simulation region is a two-dimensional rectangle, which is 11.3 mm in width and 5.6 mm in height, with an aspect ratio of 2.016. This region is surrounded by flat walls and filled with hard-sphere particles with a diameter of 3.7×10^{-10} m and a mass of 4.8×10^{-26} kg. The initial temperature and pressure are assumed to be 80 K and 20 Pa, respectively. Under these conditions, the number density is $1.81 \times 10^{22} \text{ m}^{-3}$ and the mean free path is 0.091 mm. The Knudsen number is estimated to be 0.016, which corresponds to the continuum region where the Navier-Stokes equation is valid. The simulation region is divided into 40×20 sampling cells, each of which is divided into 5×5 collision cells. Therefore, the size of the collision cell in the present simulation is smaller than the local mean free path. Initially, each sampling and collision cell contains 400 and 16 particles, respectively. The time step for the transient simulation is chosen to be 0.9 of the mean free time and a sampling is performed in every two simulation time steps. The temperature of the bottom wall is increased instantly from the initial value to a specified value at the simulation time zero and is kept constant during the simulation. The temperature of the top wall is unchanged from the initial value. The diffuse reflection is assumed at the top and bottom walls, while the specular reflection is assumed at the side walls. In the specular reflection boundary condition, the perpendicular velocity component of the incident particle is reversed, while the tangential velocity component is unchanged. It is noted that the present simulation conditions are more realistic compared with those used in the MD simulations. Only the gravitational acceleration is chosen to be a hypothetical value so that the density in the conduction state is constant throughout the simulation region [14,15]. The bottom wall temperature ranges from 100 to 500 K, and the corresponding Rayleigh number from 126 to 5341. The critical Rayleigh number of this system is about 1708, which is obtained from the linear stability analysis of the hydrodynamic equations based on the Boussinesq approximation [17]. The wavelength at the critical Rayleigh number is given as 2.016, and thus the aspect ratio of the simulation region is set equal to this value.

III. RESULTS AND DISCUSSION

The transient of the velocity field at the Rayleigh number of 4527 is shown in Fig. 1. Each velocity field is obtained by sampling particle velocities during 200 simulation steps. The statistical fluctuation is found to be approximately 0.005 during this sampling period in the present case. As is shown clearly in Fig. 1, the instant alignment of velocity vectors is observed from the bottom to the top wall, because the bottom wall temperature is instantly increased. As time develops it is seen that the velocity vector field becomes random and then two convection rolls are gradually formed. The downward flow seems to appear first at the center of the simulation region. The centers of the convection rolls are formed at mid-elevation and located close to the downward flow. In our present results, the downward flow is found to appear always in the center of the simulation region, as was seen in the hydrodynamic simulations [8]. In the MD results [11,12], on the other hand, the upward flow was observed in the center. The direction of vortices seems to be dependent on the boundary or initial conditions.

The time development of the mid-elevation temperatures near the side wall and at the center of the simulation region is shown in Fig. 2 along with the horizontal average temperature. The temperatures are normalized

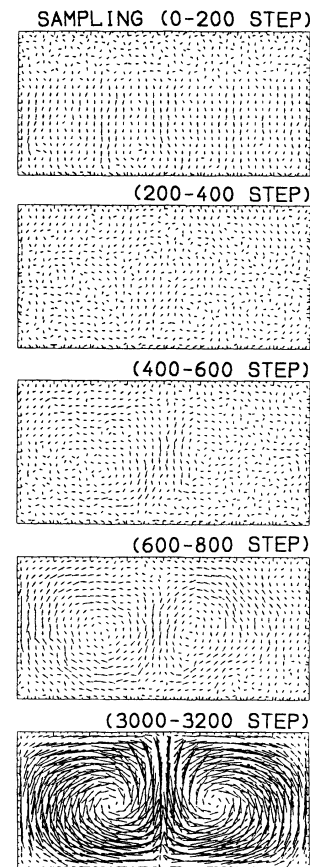


FIG. 1. Transient of the velocity field at the Rayleigh number of 4527. Each velocity vector is obtained by sampling during 200 time steps.

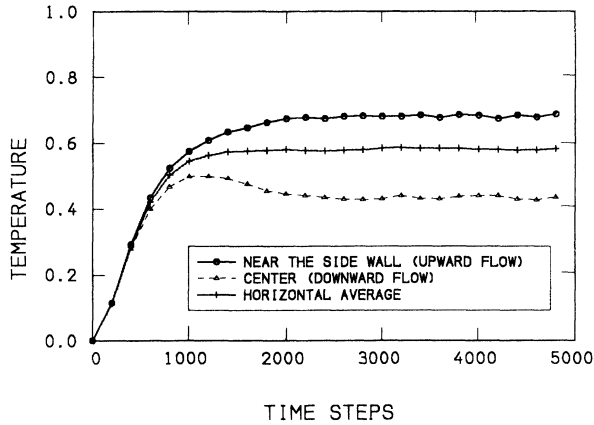


FIG. 2. Time development of the mid-elevation temperature at the Rayleigh number of 4527. The temperatures at the center and near the sidewall are shown along with the horizontal average.

so that the temperatures of the top and bottom walls are 0.0 and 1.0, respectively. The stable temperature field is found after 3000 simulation time steps. It is found that this temperature field with convection rolls remains stable even after 25 000 time steps.

The temperature and the density profiles are shown in Fig. 3 after the stable convection rolls are established. Here, a sampling is performed from 4900 to 5600 time steps. The density was normalized with the initial value. It should be noted that the contour plots shown in Fig. 3 are smeared for the density profile in particular, and the high- and low-density contours near the top and bottom walls, respectively, are not seen. However, it is found that the centers of the convection rolls shown in Fig. 1 are not on the average temperature contour of 0.5, but on the average density contour of 1.0. The high-temperature and low-density region spreads from the bottom to the

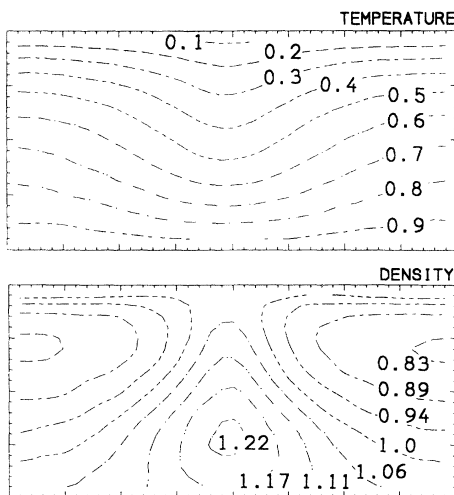


FIG. 3. Temperature and density distribution at the Rayleigh number of 4527. Sampling is performed from 4900 to 5600 time steps.

top wall along the upward flow, while the low-temperature and high-density region spreads from the top to the bottom wall along the downward flow. The temperature gradient is large near the top wall. The profiles of these macroscopic variables are similar to those obtained by the DSMC method with the semislip boundary conditions [14].

The mid-elevation temperatures near the sidewall and at the center of the simulation region are shown in Fig. 4 as a function of the Rayleigh number. This observation is made when the flow is in a complete steady state. A bifurcation between purely conductive and convective states is clearly seen at around the hydrodynamic critical Rayleigh number of 1708. In other words, the critical Rayleigh number predicted by the DSMC method, which is approximately 1700, as shown in Fig. 4, agrees with that obtained by the macroscopic hydrodynamic equations.

In our simulation, 400 particles are used in a sampling cell for all cases, and the influence of the number of simulation particles on the critical Rayleigh number is not clear. We, however, found that 40 particles in a sampling cell (1 or 2 in a collision cell) were not enough to form the vortices shown in Fig. 1 under the same conditions. There might be a necessary number of particles for simulating not only the vortices but also the transition between conduction and convection states.

The state of pure heat conduction is observed when the Rayleigh number is below this critical value, while the state of heat convection appears above the critical value. The velocity field and the temperature profile in the heat conduction state are shown in Fig. 5, where a sampling is performed between 11 700 and 12 600 time steps. The Rayleigh number in this case is 1507, which is lower than the critical value, and the convection rolls do not appear. The temperature varies almost linearly in the vertical direction, and the isothermal contour is nearly parallel to the bottom and the top walls. The mid-elevation temperature is slightly higher than 0.5, which is also seen in Fig. 4. These features of temperature distribution in the heat

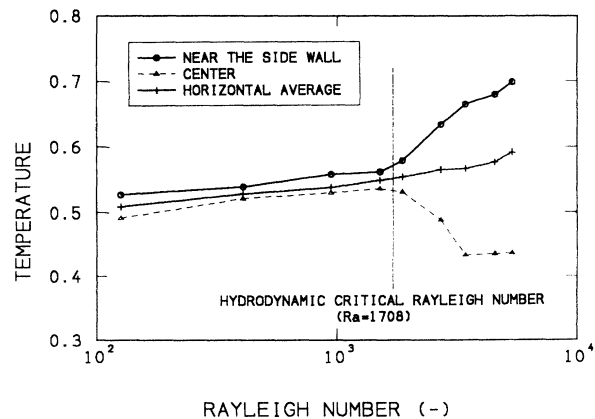


FIG. 4. Mid-elevation temperature in the steady state as a function of the Rayleigh number. The temperatures at the center and near the sidewall are shown along with the horizontal average.

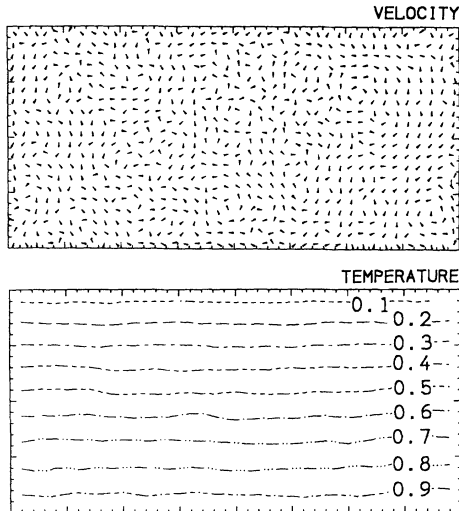


FIG. 5. Velocity field and temperature distribution at the Rayleigh number of 1507. Sampling is performed from 11 700 to 12 600 time steps.

conduction state were also observed in the MD results [9].

The midelevation temperatures obtained by using the semislip boundary condition are shown in Fig. 6. This figure corresponds to Fig. 4, in which the results by the diffuse boundary condition are shown. In our semislip simulation, the perpendicular velocity component of the reflected particle is thermalized and the transverse components are unchanged. The simulation conditions are almost the same as before except for the aspect ratio of the simulation region. The width is 15.8 mm instead of 11.3 mm, and the aspect ratio is 2.83 in this case. This aspect ratio is equal to the wavelength at the critical Rayleigh number which is obtained from the macroscopic hydrodynamic equations with the slip (inviscid) boundary condition [17].

The bifurcation between the conductive and convective states is also seen in Fig. 6, as was already shown by the diffuse boundary condition in Fig. 4. The obtained critical Rayleigh number is, however, at around 1000, while the hydrodynamic one is 658 in this case [17]. The difference in critical Rayleigh number is large compared with the former case obtained by the diffuse boundary condition. This would indicate that the semislip boundary condition does not correspond correctly to the inviscid boundary condition for the macroscopic hydro-

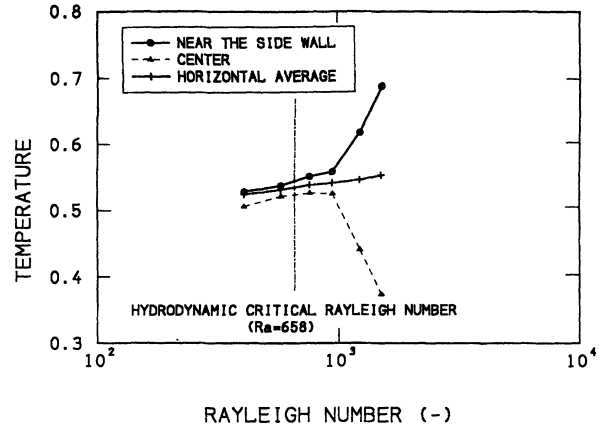


FIG. 6. Mid-elevation temperature in the steady state as a function of the Rayleigh number. The temperatures at the center and near the sidewall are shown along with the horizontal average. The semislip boundary condition is applied.

dynamic equations and is not adequate to simulate thermal boundary conditions.

IV. CONCLUSIONS

In this study the RB conduction-convection system has been simulated by using the DSMC method. The macroscopic heat conduction and convection states and the transition between these two states were simulated at the molecular level, and the results of the flow patterns were in good agreement with those derived by the hydrodynamic equations. It was found, by using the strict diffuse boundary condition at the top and bottom walls, that the determined critical Rayleigh number agreed with that of the linear stability theory. The semislip boundary condition, which had been frequently used in MD and DSMC simulations, was shown to be inadequate to simulate the thermal boundary condition. Our results suggest that the DSMC method provides a valuable tool for studying microscopic structures in macroscopic flow transitions and instabilities.

ACKNOWLEDGMENTS

One of the authors (H.K.) wishes to thank Professor B. Alder and Professor A. Garcia for informing him of their recent works.

- [1] G. A. Bird, *Molecular Gas Dynamics* (Clarendon, Oxford, 1976).
- [2] E. Meiburg, *Phys. Fluids* **29**, 3107 (1986).
- [3] G. A. Bird, *Phys. Fluids* **30**, 364 (1987).
- [4] K. Koura, *Phys. Fluids A* **2**, 209 (1990).
- [5] H. Kaburaki and M. Yokokawa (unpublished).
- [6] A. L. Garcia, *Phys. Rev. A* **34**, 1454 (1986).
- [7] See, e.g., C. W. Meyer, D. S. Cannell, and G. Ahlers, *Phys. Rev. A* **45**, 8583 (1992).

- [8] D. Mukutmoni and K. T. Yang, *Trans. ASME J. Heat Transfer* **115**, 360 (1993).
- [9] M. Mareschal and E. Kestemont, *J. Stat. Phys.* **48**, 1187 (1987).
- [10] D. C. Rapaport, *Phys. Rev. Lett.* **60**, 2480 (1988).
- [11] M. Mareschal, M. M. Mansour, A. Puhl, and E. Kestemont, *Phys. Rev. Lett.* **61**, 2550 (1988).
- [12] A. Puhl, M. M. Mansour, and M. Mareschal, *Phys. Rev. A* **40**, 1999 (1989).

- [13] J. A. Given and E. Clementi, *J. Chem. Phys.* **90**, 7376 (1989).
- [14] A. L. Garcia, in *Microscopic Simulations of Complex Flows* (Plenum, New York, 1990), p. 177.
- [15] A. Garcia and C. Penland, *J. Stat. Phys.* **64**, 1121 (1991).
- [16] S. Stefanov and C. Cercignani, *Eur. J. Mech. B Fluids* **11**, 543 (1992).
- [17] S. Chandrasekhar, *Hydrodynamic and Hydromagnetic Stability* (Clarendon, Oxford, 1916).